Human Molecular Genetics, 2009, Vol. 18, No. 24 ***4868–4878***
doi:10.1093/hmg/ddp460
Advance Access published on September 29, 2009

Defective autophagy in neurons and astrocytes from mice deficient in PI(3,5)P_2

Cole J. Ferguson, Guy M. Lenk and Miriam H. Meisler*

Department of Human Genetics, University of Michigan, Ann Arbor, MI 48109-5618, USA

Received August 10, 2009; Revised and Accepted September 25, 2009

Mutations affecting the conversion of PI3P to the signaling lipid PI(3,5)P_2 result in spongiform degeneration of mouse brain and are associated with the human disorders Charcot–Marie–Tooth disease and amyotrophic lateral sclerosis (ALS). We now report accumulation of the proteins LC3-II, p62 and LAMP-2 in neurons and astrocytes of mice with mutations in two components of the PI(3,5)P_2 regulatory complex, *Fig4* and *Vac14*. Cytoplasmic inclusion bodies containing p62 and ubiquinated proteins are present in regions of the mutant brain that undergo degeneration. Co-localization of p62 and LAMP-2 in affected cells indicates that formation or recycling of the autolysosome is impaired. These results establish a role for PI(3,5)P_2 in autophagy in the mammalian central nervous system (CNS) and demonstrate that mutations affecting PI(3,5)P_2 can contribute to inclusion body disease.

INTRODUCTION

The phosphatidylinositide PI(3,5)P_2 is a low-abundance signaling lipid that is synthesized on the cytoplasmic surface of vesicular organelles in eukaryotic cells from yeast to mammals. PI(3,5)P_2 synthesis and degradation are regulated by a protein complex that includes the PI3P kinase FAB1 (also known as PIP5K3 and PIKfyve), the Pl(3,5)P_2 5-phosphatase FIG4 and the scaffold protein VAC14 (1,2). We have described recessive mutations of human *FIG4* (also known as SAC3) in the peripheral nerve disorder Charcot–Marie–Tooth Type 4J (OMIM 611228) (3), and heterozygous deleterious mutations of *FIG4* in ~1% of patients with amyotrophic lateral sclerosis (ALS) (4). In mouse models, mutations of *Fig4* and *Vac14* result in a 50–75% reduction in the levels of PI(3,5)P_2 in cultured fibroblasts and progressive neurodegeneration that begins in fetal life and results in lethality between birth and 6 weeks of age (2,3,5). Affected mice exhibit extensive spongiform degeneration of the central nervous system (CNS) and substantial loss of peripheral neurons from sensory and sympathetic ganglia.

The PI(3,5)P_2 regulatory complex is located on the vacuolar membrane in yeast, where synthesis and degradation of Pl(3,5)P_2 are tightly coupled (2). In yeast, mutations in this regulatory complex result in reduction of PI(3,5)P_2 and enlargement of the vacuole. Mammalian cells do not contain a precise counterpart to the yeast vacuole. Mammalian FAB1 and FIG4 are associated with intracellular vesicles of the early and late endosome (6–8). In mice carrying spontaneous mutations of *Fig4* (pale tremor) and *Vac14* (ingls), the cellular concentration of PI(3,5)P_2 is reduced and there is accumulation of swollen intracellular vacuoles that appear empty of stored material in neurons and in cultured fibroblasts (2,3). Similarly, cultured fibroblasts from CMT4J patients who are deficient in FIG4 exhibit extensive cytoplasmic vacuolization (9). Treatment of mammalian cells with siRNAs to reduce expression of *Fig4* and *FAB1* also results in swollen intracellular vacuoles (10). The membrane of the enlarged vesicles in cultured fibroblasts from *Fig4* null mice stains strongly for LAMP-2, a marker of late endosomes and lysosomes (3). These previous studies have implicated PI(3,5)P_2 in the regulation of intracellular trafficking in yeast and mammalian cells.

Current models suggest that PI(3,5)P_2 is synthesized on endosomes and lysosomes in response to specific cargo molecules (10). Membrane-bound PI(3,5)P_2 is thought to interact with membrane proteins, and to recruit cytosolic effector proteins required for trafficking cargo. Through these interactions, synthesis of PI(3,5)P_2 directs trafficking of cargo vesicles along the endosome–lysosome axis and promotes recycling of membranes to the *trans*-Golgi network (7).

*To whom correspondence should be addressed at: Department of Human Genetics, University of Michigan Medical School, 4909 Buhl, Ann Arbor, MI 48109-5618, USA. Tel: +1 7347635546; Fax: +1 7347639691; Email: meislerm@umich.edu

Macroautophagy (autophagy) is a ubiquitous eukaryotic pathway for degrading damaged organelles and long-lived intracellular proteins (11). Autophagy provides nutrients during periods of starvation and serves as a quality control mechanism for misfolded proteins. During autophagy, ubiquitin-tagged substrates are sequestered within double-membrane vesicles that are thought to be enriched in PI3P, the precursor of $PI(3,5)P_2$ (12). Completed autophagosomes can fuse directly with lysosomes, or with endosomal vesicles prior to lysosome fusion, in order to deliver substrates for degradation. In yeast, reduction of $PI(3,5)P_2$ does not appear to affect autophagy (10). In mammalian cells, autophagy is dependent on maturation of early endosomes (13). In view of the established role of $PI(3,5)P_2$ in endosomal trafficking, we hypothesized that reduced levels of $PI(3,5)P_2$ might affect the progression of autophagy in mammalian cells, and that the resulting impairment of autophagy could be responsible for the extensive neurodegeneration in the $PI(3,5)P_2$-deficient mutants *Fig4* (pale tremor) and *Vac14* (ingls).

The work described here directly tests the hypothesis that there is a block in autophagy in *Fig4* and *Vac14* mutant mice. Our data support and extend the evidence that $PI(3,5)P_2$ is an essential component of the autophagy pathway. We demonstrate that impaired autophagy underlies neurodegeneration in these mutant mice and is likely to contribute to related human disorders.

RESULTS

Autophagy markers in *Fig4*$^{-/-}$ brain

p62/SQSTM1 binds polyubiquinated protein substrates destined for autophagic degradation. Using western blotting, we assessed the amount of p62 in *Fig4*$^{-/-}$ null mice. A significant increase in abundance of p62 was observed in brain and spinal cord (Fig. 1A). The abundance of p62 in 10 μg of mutant brain is comparable with that in 30 μg of wild-type brain, indicating that p62 is increased 3-fold in the mutant (Fig. 1A). Analysis of brain RNA by qRT-PCR demonstrated that the level of p62 transcript is not elevated (Fig. 1B). p62 accumulation is limited to brain and spinal cord, and was not observed in liver or other non-neural tissues (Fig. 1C).

LC3-II (MAP1LC3), a component of the autophagosome membrane that binds p62, is generated by conjugation of phosphatidylethanolamine to the cytosolic protein LC3-I, resulting in faster electrophoretic mobility. Elevated LC3-II, but not LC3-I, is a consequence of defective autophagosome clearance (14). Examination of brain homogenates by western blotting demonstrated an increase in the level of LC3-II in the *Fig4*$^{-/-}$ mutant (Fig. 1D). There is no change in cytoplasmic LC3-I (Fig. 1E). The increased levels of p62 and LC3-II indicate that the process of autophagy is altered in $PI(3,5)P_2$-deficient *Fig4*$^{-/-}$ mice.

Autophagy is not up-regulated in mutant brain

The accumulation of LC3-II could result either from an elevated rate of basal autophagy, as observed in some lysosomal storage disorders, or from a block in the completion of autophagy. To distinguish between these, we examined the abundance of several proteins involved in the initiation of autophagy. Beclin-1 is a subunit of the class III PI3-kinase complex that is required for autophagosome formation. In *Fig4*$^{-/-}$ brain, the level of beclin-1 protein was comparable to that of wild type (Fig. 2A). Mammalian target of rapamycin (mTOR) is an important regulator of autophagy that is elevated in some lysosomal storage disorders. In mutant brain, we observed normal levels of Ser2448-phosphorylated and total mTOR (Fig. 2B and C). We also examined phosphorylated p70 S6 kinase (p-S6K), an intermediate in regulation by mTOR. The level of p-S6K was normal in the mutant brain (Fig. 2D). These data indicate that the accumulation of autophagy intermediates in *Fig4*$^{-/-}$ brain is likely to result from a block in completion of basal autophagy rather than up-regulation of the pathway.

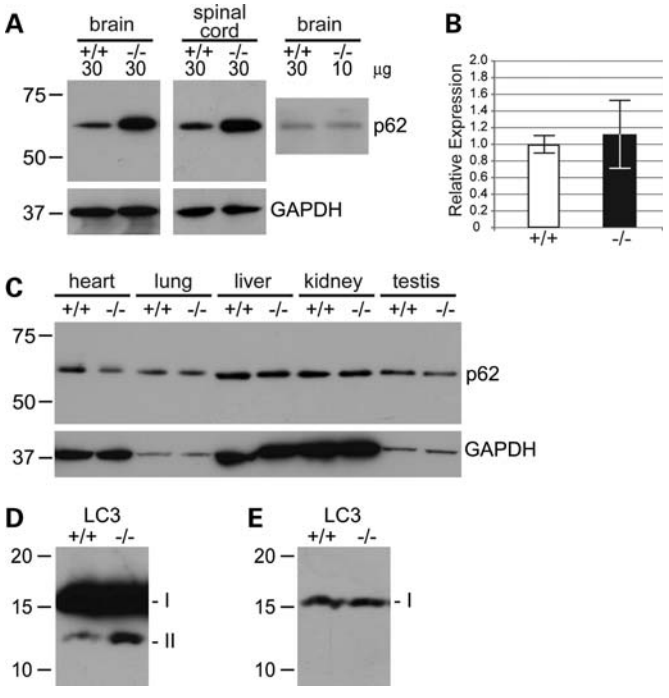

Figure 1. Markers of autophagy are elevated in brain from *Fig4*$^{-/-}$ brain. Total brain homogenates were examined by western blotting with antibodies to components of the autophagy pathway. (**A**) Accumulation of p62 in mutant brain and spinal cord (left and middle panels); quantitative comparison (right panel). (**B**) qRT-PCR analysis of p62 transcript, relative to the Tata-binding protein transcript, in total brain RNA. Mean ± SD ($n = 3$ mice of each genotype, assayed in quadruplicate). (**C**) Normal levels of p62 protein in non-neural tissues. (**D**) Elevation of LC3-II in mutant brain. (**E**) Normal level of LC3-I in mutant brain [short exposure of the film in (D)]. (A)–(C) 30 μg protein per lane; (D)–(E) 50 μg protein per lane.

p62 and ubiquitin in inclusion bodies

Insoluble protein aggregates containing p62 and ubiquitin are a common feature of several types of neurodegenerative disease (15). To determine whether the elevated p62 in *Fig4*$^{-/-}$ brain is associated with ubiquitinated protein, brain slices were immunostained for p62 and ubiquitin. Co-localization of p62 and ubiquitin was evident in sections of the cortex (Fig. 3A) and other regions of the brain. Both

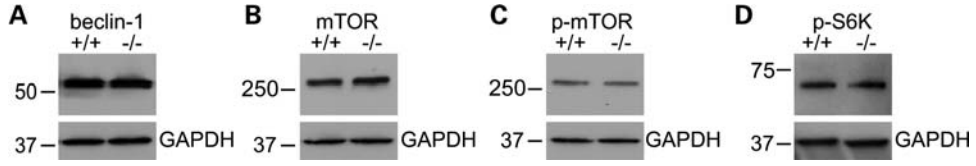

Figure 2. Normal levels of proteins involved in initiation and mTOR-mediated regulation of autophagy. (**A**) beclin-1; (**B**) mTOR; (**C**) Ser2448 phospho-mTOR; (**D**) phosphorylated p70 S6 kinase, a downstream target of mTORC1. Thirty micrograms of protein per lane.

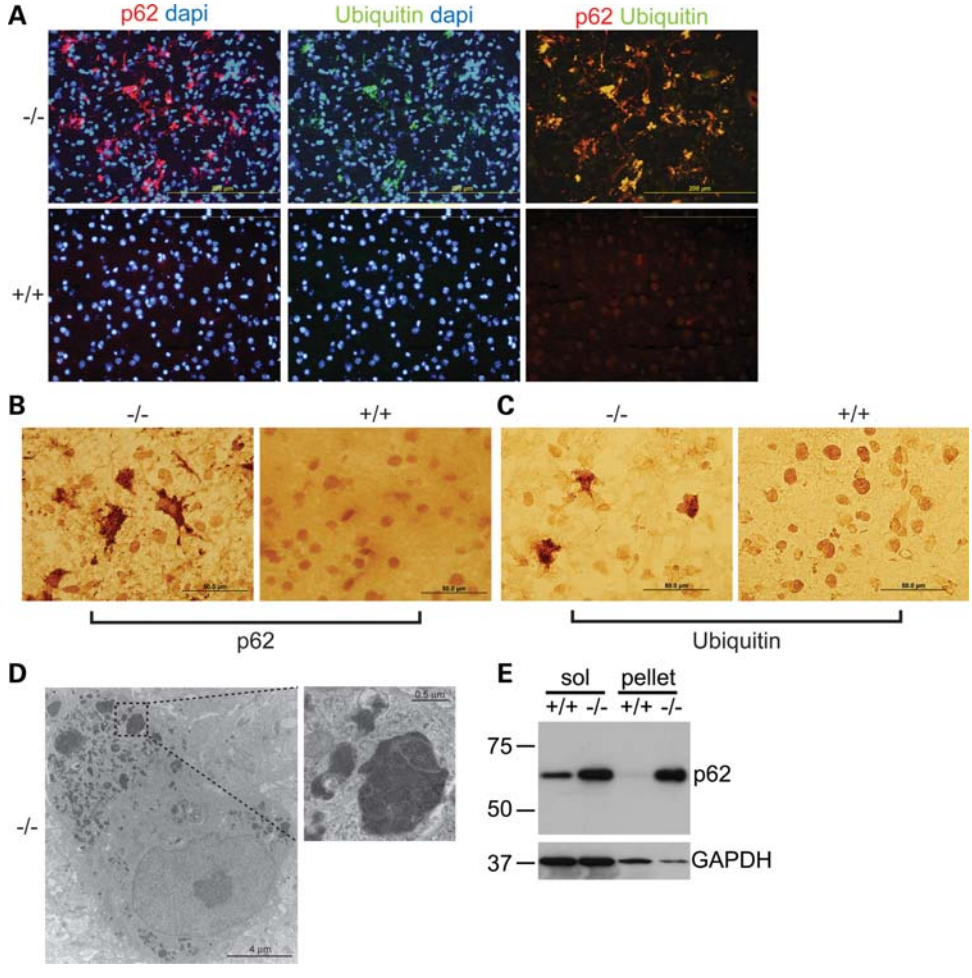

Figure 3. p62 is co-localized with ubiquitin in intracellular inclusion bodies. (**A**) Two-color immunofluorescence of cortical sections from *Fig4*$^{-/-}$ mouse demonstrates co-localization of ubiquitin and p62. (**B** and **C**) Peroxidase immunostaining detects immunodense cytoplasmic inclusion bodies containing p62 and ubiquitin in mutant brain that are not present in wild-type controls. (**D**) Ultrastructure (TEM) of *Fig4*$^{-/-}$ brainstem at 7 days of age. (**E**) Western blot of soluble protein and 15 000*g* pellet from brain homogenates prepared in radioimmunoprecipitation buffer. Thirty micrograms of protein per lane.

p62 and ubiquitin are associated with densely stained intracellular inclusions that sometimes extended into cell processes (Fig. 3B and C). Ultrastructural analysis of the brainstem revealed numerous electron-dense cytoplasmic vesicles that range in diameter from 0.25 to 4 μm (Fig. 3D) and resemble those in other neurodegenerative disorders (15). Consistent with localization of p62 in inclusion bodies, a significant proportion of p62 is pelleted by centrifugation of mutant brain homogenates at 15 000*g* (Fig. 3E).

Inclusion bodies do not contain TDP-43

In some forms of ALS, the nuclear DNA-binding protein TDP-43 is co-localized in cytoplasmic inclusion bodies that contain p62 and ubiquitin (16–18). We did not detect any increase in TDP-43 protein in *Fig4*$^{-/-}$ brain by western blot (Supplementary Material, Fig. S1A). Immunostaining revealed normal nuclear localization of TDP-43 (Supplemental Material, Fig. S1B), and lack of co-localization with

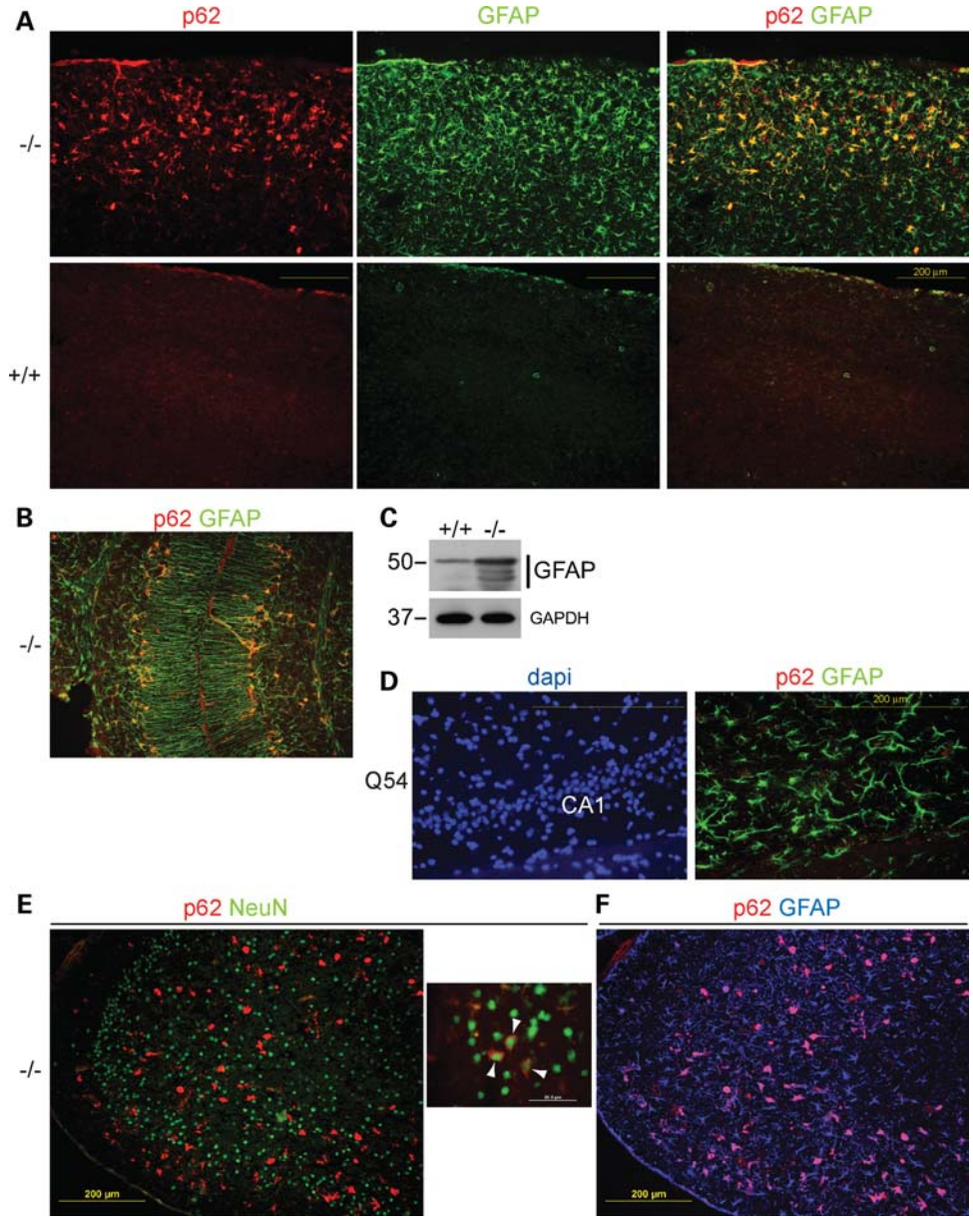

Figure 4. Accumulation of p62 in reactive astrocytes and neurons of *Fig4*$^{-/-}$ brain. (**A**) Immunostaining of cortical sections demonstrates co-localization of p62 and GFAP, an astrocyte marker. (**B**) p62 accumulation in GFAP-positive Bergmann glia in mutant cerebellum; see also Supplementary Material, Fig. S2. (**C**) Western blot demonstrates increased abundance of full-length GFAP and degradation products in mutant brain; 30 μg protein per lane. (**D**) Lack of p62 accumulation in astrocytes in the CA1 region of the hippocampus from *Fig4*$^{+/+}$ epileptic brain. (**E**) Neurons were identified with antibody to the nuclear marker NeuN. Only a small number of NeuN-labeled nuclei are associated with cytoplasmic p62 (insert, arrowheads). (**F**) Most of the p62 in this section is localized in GFAP-positive astrocytes, as also seen in (A).

cytoplasmic p62 (Supplementary Material, Fig. S1C). The data indicate that TDP-43 is not involved in the neuropathology in *Fig4*$^{-/-}$ mice.

Astrocytes exhibit high levels of p62

To identify the cells containing p62 in *Fig4*$^{-/-}$ brain, we co-immunostained brain sections for p62 and cell-specific markers. Extensive overlap was observed when cortical sections were stained for p62 and the astrocyte marker GFAP (glial fibrillary acidic protein) (Fig. 4A). In wild-type brain, the levels of p62 and GFAP were low and no overlap was detected. In mutant cerebellum, immunostaining detected high levels of p62 in Bergmann glia (Fig. 4B and Supplementary Material, Fig. S2). These cells reside at the border between the molecular and granule cell layers of the cerebellum and their projections extend to excitatory synapses of the Purkinje cell dendritic arbor. Consistent with the intensity of immunostaining, western blotting demonstrated significant accumulation of both full-length and degraded GFAP (Fig. 4C).

To investigate the temporal relationship between spongiform degeneration and the appearance of p62-containing astrocytes, we examined *Fig4*$^{-/-}$ brain at 1 week of age, when a small

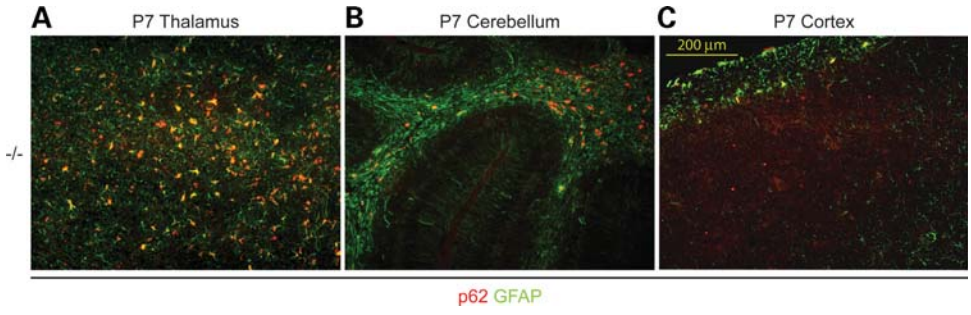

Figure 5. p62-containing astrocytes in *Fig4*$^{-/-}$ brain at 1 week of age. (**A**) Accumulation of p62 in GFAP-positive astrocytes in the thalamus, which exhibits spongiform degeneration at 1 week of age (3). (**B**) Accumulation of p62 in white matter tracts around the cerebellar nuclei, a site of extensive spongiform degeneration in older animals. (**C**) The cortex is unaffected at P7 (3).

amount of degeneration is visible in the thalamus and brain stem but not in cortex (3). Co-staining of p62 and GFAP was evident in the thalamus, but not in the cortex (Fig. 5 and Supplementary Material, Fig. S3). p62-positive astrocytes were also present in the axonal tracts near the cerebellar nuclei (Fig. 5), a region that is severely affected at later stages (3) (Supplementary Material, Fig. S3). Thus, the appearance of p62-positive astrocytes accompanies the earliest signs of neurodegeneration, consistent with a primary role in pathogenesis.

As a control for the specificity of p62 accumulation in *Fig4*$^{-/-}$ astrocytes, we examined *Fig4*$^{+/+}$ astrocytes in Q54 mice, a model of temporal lobe epilepsy with hippocampal sclerosis (19). Intensely staining GFAP-positive astrocytes are present in the CA1 region of Q54 hippocampus, but these astrocytes do not contain high levels of p62 (Fig. 4D). Thus, p62 accumulation is not a general feature of astrocytosis, but is specific to *Fig4*$^{-/-}$ brain.

p62 in neurons and other types of glia

To assess the accumulation of p62 in neurons, brain slices were co-stained for p62 and NeuN, a marker of neuronal nuclei. A small number of neurons contain cytoplasmic p62 surrounding the NeuN-positive nucleus (Fig. 4E, insert). However, the major portion of p62 staining is in astrocytes (Fig. 4F), as also discussed above.

Oligodendrocytes were identified by *in situ* hybridization with a cDNA probe for MAG (myelin-associated glycoprotein). MAG-positive cells did not contain p62 (Supplementary Material, Fig. S4B). Microglia were identified by immunostaining with the marker Iba1. Numerous microglia were present in mutant brain, suggestive of activation by ongoing neuronal damage (Supplementary Material, Fig. S4B). However, there was no overlap of immunostaining for Iba1 and p62. Thus, the major site of p62 accumulation is in astrocytes, with a small contribution from neurons.

Co-localization of LAMP-2 and p62 in astrocytes

LAMP-2 is a highly glycosylated membrane protein that is localized to vesicles of the late endosome and lysosome (20). We previously demonstrated the presence of LAMP-2 in the limiting membrane of the cytoplasmic vacuoles in cultured fibroblasts from *Fig4*$^{-/-}$ mice (3). Western blot analysis of total brain homogenate revealed significant elevation of LAMP-2 in mutant brain (Fig. 6A). The abundance of LAMP-2 in 10 μg of mutant brain is comparable with that in 30 μg of wild-type brain (Fig. 6A). The elevation of LAMP-2 is thus ∼3-fold, similar to the elevation of p62 (Fig. 1A).

To determine which cells accumulate LAMP-2, we co-stained cortical sections for LAMP-2 and cell-specific markers. The majority of LAMP-2 staining was localized to GFAP-positive astrocytes (Fig. 6B). LAMP-2 is thus accumulating in the same cells that accumulate p62 and ubiquinated protein (Figs 3 and 6). High magnification confocal imaging demonstrated co-localization of p62 and LAMP-2 in intracellular vesicles (Fig. 6D).

LAMP-2 positive vesicles in cultured *Fig4*$^{-/-}$ neurons

We previously described neuronal vacuolization in sensory ganglia, thalamus, brain stem and ventral spinal cord of *Fig4*$^{-/-}$ brain (3). Because only a few vacuolized neurons are visible in brain sections, we examined LAMP-2 staining of neuronal vacuoles using cultured neurons. Cerebellar granule cells were isolated from *Fig4*$^{-/-}$ mice at postnatal day 3 and cultured for 11 days as described (21). Approximately 25% of the cultured neurons exhibit extensive vacuolization with LAMP-2 staining of vacuoles. In the most severely affected neurons, vacuoles filled the soma and neuronal processes (Fig. 6E). The dramatic appearance of these cells suggests that the first step in pathogenesis may be neuronal cell death due to extensive vacuolization, followed sequentially by a defective astrocyte response and spongiform degeneration.

Abnormal autophagy in *Vac14* mice mutant

VAC14 is a component of the PI(3,5)P_2 regulatory complex that acts as a scaffold protein and binds directly to FIG4 and the kinase FAB1 (Fig. 7A). The *Vac14*^{L156R} mutation in the mouse mutant *ingls* disrupts the interaction with FAB1, resulting in reduced PI(3,5)P_2 and neurodegeneration that mimic the *Fig4*$^{-/-}$ phenotype (2). We therefore examined the *ingls* mouse as an independent test of the hypothesis that reduced PI(3,5)P_2 leads to abnormal autophagy.

Examination of brain homogenates by western blotting demonstrated elevated levels of both p62 and LC3-II in *ingls* brain (Fig. 7B). The p62 is co-localized with ubiquitin in brain sections from the *ingls* mouse (Fig. 7C). Numerous acti-

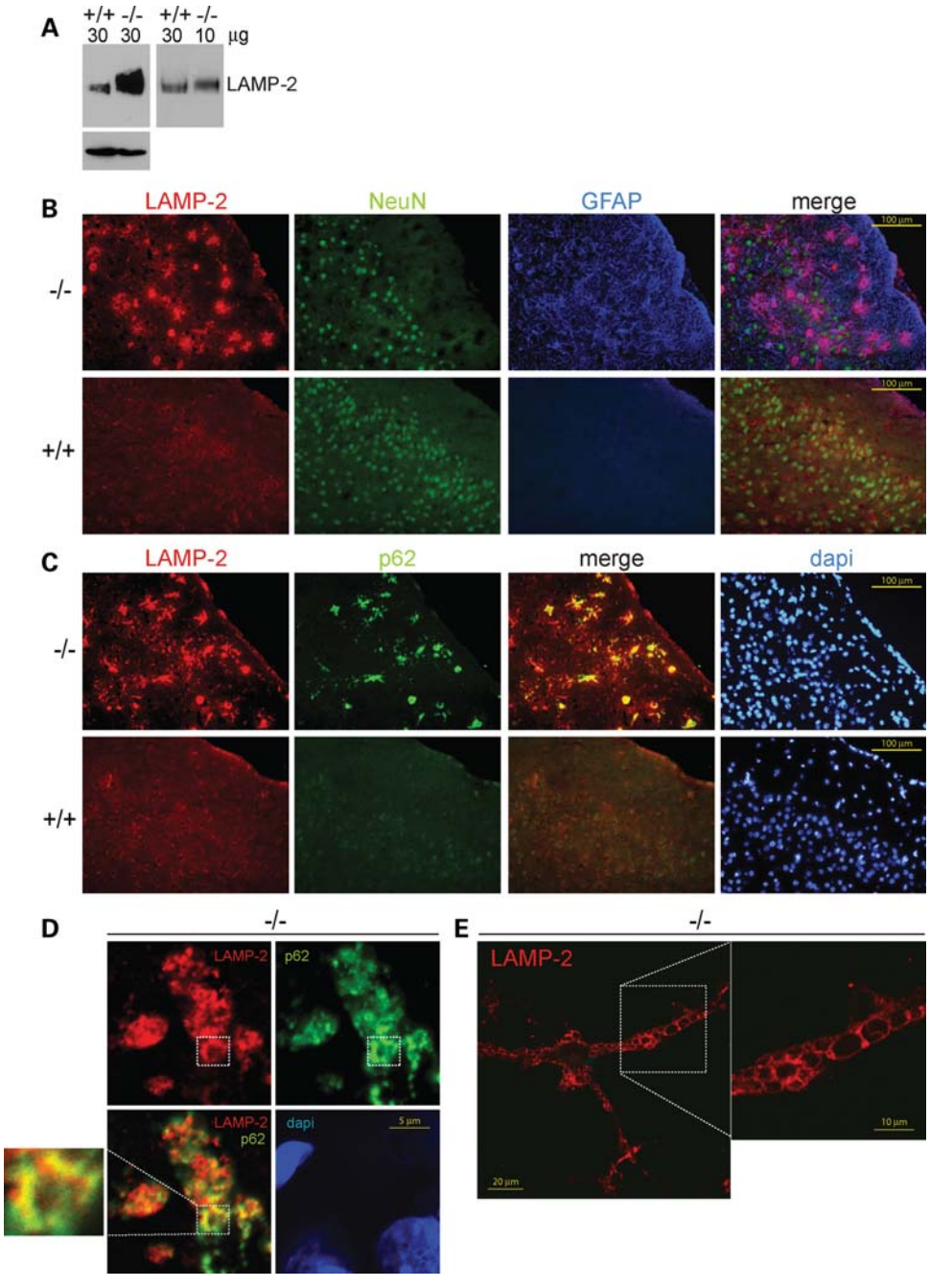

Figure 6. Accumulation of LAMP-2 in *Fig4*$^{-/-}$ brain. LAMP-2 is a major component of lysosomal membranes, and is also present in late endosomes and autophagosomes. (**A**) Western blot demonstrates accumulation of LAMP-2 in mutant brain (left panel) with quantitative comparison (right panel). (**B**) LAMP-2 is concentrated in GFAP-positive astrocytes and not in NeuN-poistive neurons. (**C**) Co-localization of LAMP-2 and p62. (**D**) High-resolution confocal imaging (×180) demonstrates subcellular co-localization of LAMP-2 and p62. (**E**) In cultured cerebellar granule neurons from *Fig4*$^{-/-}$ mice, soma and processes (insert) are filled with LAMP-2-positive vacuoles.

vated astrocytes containing p62 were detected by immunostaining (Fig. 7D). A small proportion of neurons in the *ingls* brain was positive for p62 (Fig. 7D, insert, arrowheads). LAMP-2 is also elevated in *ingls* brain (Fig. 7E). Overall, the accumulation and cellular location of autophagy markers in the *ingls* mutant closely resembles those of *Fig4*$^{-/-}$ mice, supporting the view that the deficiency of PI(3,5)P_2 is responsible for defective autophagy and neurodegeneration in both mutants.

DISCUSSION

Autophagy and PI(3,5)P_2

In yeast, mutations of the PI(3,5)P_2 regulatory complex result in enlargement of the vacuole organelle, but do not interfere with autophagy (10). However, in *Drosophila* and in *Caenorhabditis elegans*, mutation of the *FAB1* component of the regulatory complex led to accumulation of the LC3 homologs (22,23),

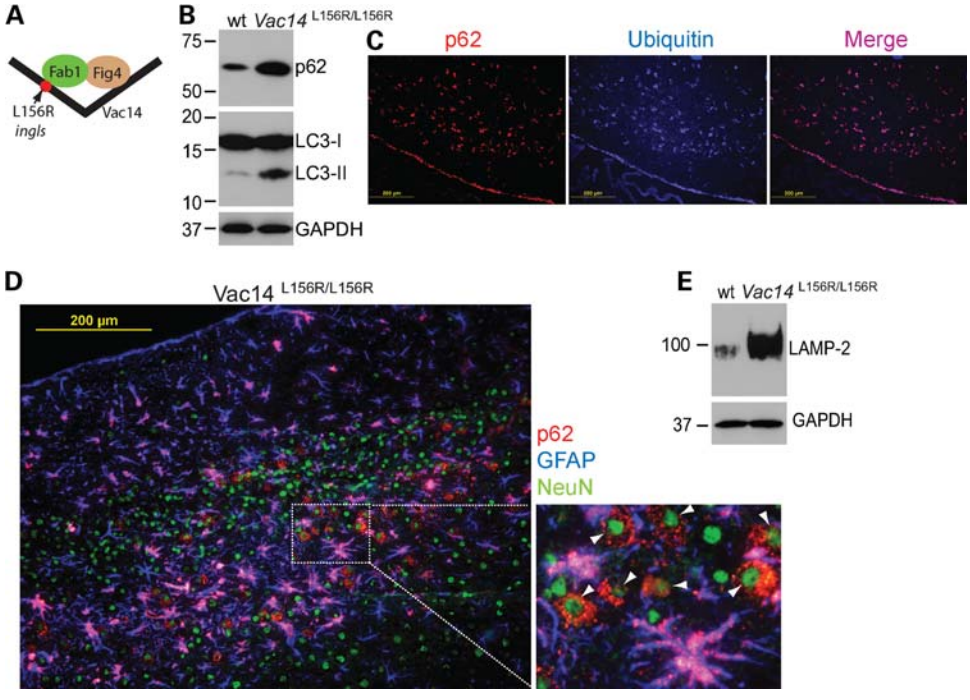

Figure 7. Impaired autophagy and astrocytosis in a second mouse mutant affecting $PI(3,5)P_2$. (**A**) The protein VAC14 binds FIG4 and FAB1 kinase in the molecular complex that regulates $PI(3,5)P_2$ synthesis. The Vac14-L156R mutation (red) in the *ingls* mutant mouse results in destabilization of the complex and reduced levels of $PI(3,5)P_2$ (2). (**B**) Elevated levels of p62 and LC3-II in brain homogenates from Vac14-mutant mice. Each lane contains 30 μg of protein. (**C**) Co-localization of p62 and ubiquitin in *ingls* cortex. (**D**) Accumulation of p62 in astrocytes and neurons. (**E**) Accumulation of LAMP-2 in *ingls* brain; 30 μg protein per lane.

indicating that this pathway has diverged between yeast and higher organisms. The present report is directed toward the role of $PI(3,5)P_2$ signaling in mammalian autophagy *in vivo*. In two independent mouse mutants deficient in $PI(3,5)P_2$, elevated levels of the autophagy markers LC3-II and p62, were detected in brain. Induction of autophagic flux is often accompanied by elevation of LC3-II levels and reduced levels of p62 (24). In mutant brain, the level of p62 is greatly *increased* and several proteins involved in regulation of autophagy are not altered. These observations indicate that the predominant effect of deficient $PI(3,5)P_2$ is to block the progression of autophagy. This view is supported by the recent observation that inhibition of FAB1 in cultured cells results in accumulation of LC3-II (25). Our data do not rule out the possibility that there may also be some mTOR-independent induction of basal autophagy.

The accumulated p62 in mutant brain is located in insoluble inclusion bodies that also contain ubiquitinated protein. Inclusion bodies containing p62 and ubiquitin are characteristic of several types of neurodegenerative disease (26). It is clear that nervous system is particularly susceptible to reduction of $PI(3,5)P_2$ *in vivo*, since other tissues do not exhibit cellular vacuolization or accumulation of autophagy intermediates.

Two models for the specific role of $PI(3,5)P_2$ in autophagy may be considered (Fig. 8). In the first model, $PI(3,5)P_2$ is located on the membranes of autophagosomes, late endosomes and/or lysosomes, where it serves as a molecular signal for vesicle fusion leading to mature autolysosomes. Deficiency of $PI(3,5)P_2$ on these membranes could slow or prevent vesicle fusion events (Fig. 8-1), leading to accumulation of

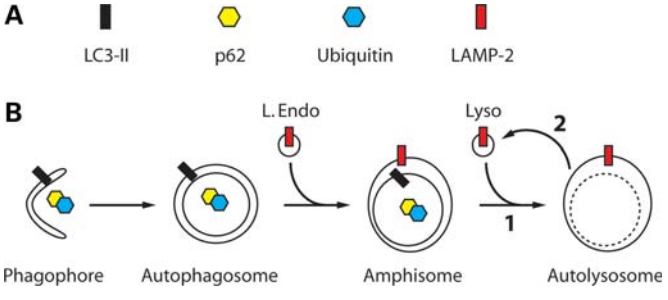

Figure 8. Schematic depiction of maturation and resolution of the autophagosome. (**A**) Proteins that accumulate in brain of pale tremor (*Fig4*) and ingls (*Vac14*) mutant mice. (**B**) Model of maturation of autophagic vesicles, with two potential sites of slowdown or blockage that could explain the accumulation of autophagosome and lysosome marker proteins.

vesicles containing p62. An alternate model is that $PI(3,5)P_2$ is required for recycling of the autolysosome membrane after fusion of the amphisome with the lysosome (Fig. 8-2). In this model, autophagy intermediates could accumulate due to the deficiency of membrane components required for continued generation and maturation of autophagosomes. The second model is comparable with the effect of $PI(3,5)P_2$ deficiency in yeast, where the enlarged vacuole appears to result from failure of vacuole fission and budding (10). The second model is supported by the co-localization of p62 with LAMP-2, which implies that vesicle fusion has occurred. The two alternative models are not mutually exclusive, and both steps may be impaired in $PI(3,5)P_2$-deficient mice. The progression of autophagy in the mutant mice may be only par-

tially blocked, since mutant fibroblasts contain residual $PI(3,5)P_2$ and many tissues, including liver, do not exhibit degeneration (2). Definitive understanding of the role of $PI(3,5)P_2$ in this pathway will require more detailed information regarding the precise localization of $PI(3,5)P_2$ and its regulatory complex in mammalian cells.

Roles of neurons and astrocytes

Accumulation of membrane-bounded vesicles in neurons of the CNS and peripheral nervous system was found to be an early feature of neurodegeneration in *Fig4* and *Vac14* mutant mice (2,3). The current work demonstrates that the majority of accumulated p62 in mutant brain is located within astrocytes. Astrocytes comprise a majority of cells in the CNS, and regulate reuptake of glutamate from excitatory synapses and response to neuronal injury (27). Abnormal astrocytes are present as early as 1 week of age, specifically in brain regions that later exhibit the greatest degeneration. Thus, both neurons and astrocytes are affected early in disease progression, and conditional inactivation will be required to separate their contributions. The data are consistent with a model of pathogenesis in which the initiating event is vesicle accumulation and death of neurons, followed by recruitment of astroctyes which are unable to respond adequately to the injury, leading to local neurotoxicity and generation of the empty spaces characteristic of spongiform degeneration. This model is supported by the dramatic accumulation of LAMP-2-positive vacuoles in soma and processes of neurons in culture. The small number of p62-positive neurons visible in brain sections may reflect the short survival time of neurons after the start of vacuolization. The vulnerability of neurons may be related to their postmitotic state, since accumulated vesicles are not diluted by distribution to daughter cells during cell division. The high level of membrane turnover in neurons is thought to contribute to the unique dependence of neurons on autophagy.

Astrocytes and Bergmann glia in the *Fig4* and *Vac14* mutant brains exhibit morphological features of activation such as hypertrophy, elongated processes, and high GFAP content. The detection of increased GFAP on western blots of whole brain homogenates demonstrates the high level of astrocytosis in the degenerating brains. p62 accumulates in astrocytes of *Fig4* or *Vac14* mutant mice, but not in a model of seizure-induced astrocytosis.

The relative contribution of neurons and astrocytes to the development of ALS has been evaluated in the mouse model of SOD1-dependent ALS. Both *FIG4* and *SOD1* are ubiquitously expressed 'housekeeping genes' in which certain missense mutations result in late-onset neurodegenerative disease. p62/ubiquitin inclusion bodies are observed in both neurons and astrocytes of mice carrying ALS-associated mutations of SOD1. Global expression of mutant SOD1 transgenes in the mouse recapitulates the human disease, but tissue-specific transgene expression in astrocytes does not itself induce disease (28). Tissue-specific expression in neurons is pathogenic if expression is sufficiently high (29,30). Using conditional knock-out technology, tissue-specific knock-out of mutant SOD1 expression in astrocytes was shown to delay disease progression (31). Recapitulation of the SOD1 mutant phenotype requires interaction between neurons, astrocytes, microglia and, possibly, other cell types. In $Fig4^{-/-}$ mice, affected cells include neurons, astrocytes, and Schwann cells (3,9). Future application of the conditional knock-out approach will permit dissection of the contributions of these and other cell types to $PI(3,5)P_2$-deficient neuropathology.

Autophagy and neurological disease

The combination of p62/ubiquitin-positive inclusion bodies and neurodegeneration may result from three distinct categories of gene mutations. The most extensively studied are dominantly inherited mutations in substrates of autophagy that produce 'toxic' proteins that accumulate because they are resistant to degradation. Examples include LRRK2 and PARKIN in Parkinson's disease, SOD1 and TDP-43 in ALS, and the expanded polyglutamine repeat-containing huntingtin protein. In these cases, the mutant protein is a major component of the inclusion bodies, and accumulation of the mutant protein is the cause of degeneration.

The lysosomal diseases represent a second category of neurodegeneration with p62/ubiquitin inclusion bodies. In these disorders, mutation of a lysosomal enzyme or ion-channel interferes with protein degradation, resulting in back-up accumulation of autophagy intermediates (32). Up-regulation of the autophagy pathway is observed in these disorders, apparently as an attempt to compensate for the accumulation of non-degraded proteins.

We propose that mutations that directly affect components of the autophagy machinery may be considered a third category of inclusion-body-related neurodegenerative disease, and that the *Fig4* and *Vac14* mutations affecting $PI(3,5)P_2$ fall into this category. Accumulation within neurons of proteins that are normally degraded by autophagy is likely to mediate neuronal cell death. Neuron-specific inactivation of the autophagy proteins ATG5 and ATG7 generates a pattern of neurodegeneration and accumulation of p62/ubiquitin inclusion bodies very similar to those described here (33,34). Other neurodegenerative disorders that may directly affect autophagy are Chorea acanthocytosis due to mutation of the endosomal protein Soi3 (VPS13a), which interacts with FAB1 (35,36), and ALS with Frontotemporal Dementia due to mutation of the CHMP2B subunit of the ESCRT complex (37,38).

p62/ubiquitin inclusion bodies are a hallmark of ALS. Detection of p62/ubiquitin inclusions in *Fig4*-deficient mice supports our recent report that heterozygosity for partial or complete loss-of-function alleles of *FIG4* may be a risk factor for ALS (4). The importance of autophagy in ALS pathogenesis is also supported by recent evidence that increasing autophagy *via* XBP-1 deficiency protects against SOD1-induced ALS in the mouse (39).

The current work suggests that defective autophagy is a potential target for treatment of patients with mutations in *FIG4*. Induction of autophagy is also protective against the toxicity of mutant huntingtin in cultured neurons and *in vivo* (40,41). Long-term *in vivo* treatment with rapamycin, another inducer of autophagy, is well tolerated in the mouse

and leads to extended lifespan (42). Drugs that increase the abundance of PI3K may induce autophagy in part by increasing the substrate for conversion of PI3P to $PI(3,5)P_2$. In addition to suggesting therapeutic approaches, our observations indicate that other genes encoding components of the autophagy machinery should be evaluated for their role in inherited neurodegenerative disorders.

MATERIALS AND METHODS

Animals

The pale tremor mutant, *Fig4*$^{-/-}$, is derived from a spontaneous mutant that arose on a mixed inbred background (3). *Fig4*$^{-/-}$ mice are maintained as a recombinant inbred strain that was derived from an F2 cross with strain CAST/EiJ. The line is maintained by brother × sister mating of heterozygous carriers, and is now at generation N10. The *ingls* mutant (infantile gliosis) carrying the Vac14^{L156R} mutation arose on strain DBA/2J and is maintained as a congenic line on strain C57BL/6J (2). The congenic line B6.D2-*Vac14*^{ingls}/J (N23) was obtained from the Jackson Laboratory (stock number 003095). Experiments were carried out on *Fig4*$^{-/-}$ mice between 3 and 4 weeks of age, unless otherwise indicated, and *ingls* mice at 2 weeks of age. The Q54 mice with temporal lobe epilepsy due to a mutation in sodium channel *Scn2a* are maintained on the C57BL/6J background (N15) (19). Frozen brain from affected Q54 (B6.Q54XSJL/J)F1 mice was provided by Jennifer Kearney (Vanderbilt University). Animals were housed and cared for in accordance with NIH guidelines, and experiments were approved by the University of Michigan Committee on Use and Care of Animals.

Western blot analysis

Tissue homogenates (10%, weight/volume) were prepared by homogenization with a Polytron homogenizer in radioimmunoprecipitation (RIPA) buffer (150 mM NaCl, 1% NP-40, 1% sodium deoxycholate, 0.1% SDS in 25 mM Tris, pH 7.5) containing complete EDTA-free protease inhibitor cocktail (Roche) and 1:1000 β-mercaptoethanol. Homogenates were centrifuged at 15 000*g*. Protein concentration was determined in triplicate using the bicinchoninic acid protein assay reagent (Pierce Chem.) Pellets were resuspended in RIPA buffer using the Polytron homogenizer. Samples were boiled for 3 min in the presence of β-mercaptoethanol prior to electrophoresis on precast 4–20% SDS-PAGE gels (Criterion) and transfer to Hybond nitrocellulose membranes (Amersham Biosciences). Membranes were pre-incubated for 1 h at room temperature in western blocking solution, 1% BSA fraction V (Fischer Scientific) with 5% powdered milk (Amresco) in TBST (Tris-buffered saline with Tween 20). Primary antibody incubation was carried out overnight at 4°C. Guinea pig anti-p62 (American Research Products) was used at 1:1000, rabbit anti-LC3 (Novus Biologicals) at 1:500, anti-TDP-43 (Proteintech Group) at 1:500, rat anti-LAMP2 (ABL-93 concentrate fraction, Iowa Hybridoma bank) at 1:1000, rabbit anti-GFAP (Abcam) at 1:1000, rabbit anti-Beclin-1 (Santa Cruz) at 1:1000 and rabbit anti-mTOR (Cell Signaling) at 1:1000. Membranes were blocked in 3% BSA prior to staining with mouse anti-GAPDH (1:30,000, Abcam), rabbit anti phospho-p70S6 kinase (1:250, Cell Signaling) and rabbit phospho-mTOR Ser2448 (1:1000, Cell Signaling). Membranes were washed in TBST and incubated with peroxidase-labeled secondary antibodies for 1 h at room temperature. Chemiluminescence was detected with the Supersignal West Femto chemiluminescence reagent (Pierce) and Hybond-CL autoradiography film (Denville Scientific).

Quantitation of p62/SQSTM1 mRNA

RNA was extracted from whole brain ($n = 3$ for each genotype) using the TriZol reagent (Invitrogen). cDNA was generated using oligo-dT primers with the SuperScript first-strand synthesis RT-PCR kit (Invitrogen). Expression was measured using predesigned TaqMan assay probes (www.appliedbiosystems.com) with analysis on a StepOne Plus real-time PCR system (ABI). Each sample was assayed in quadruplicate and expression of p62/SQSTM1 was normalized to the Tata binding protein (*Tbp*).

Immunocytochemistry

Fresh frozen saggital cryosections (10 μm) were dried at room temp for 20 min, fixed in fresh 3.2% paraformaldehyde (Pierce) for 20 min, permeabilized with 0.2% Triton X-100 and blocked in 10% goat serum. Primary antibody to p62 (1:200 mouse anti-p62, Abnova H00008878-M01) or ubiquitin (or 1:200 rabbit anti-ubiquitin, DAKO) was applied and sections were incubated overnight at 4°C in 5% goat serum. Peroxidase-diaminobenzidine staining was carried out with the Histostain kit (Zymed). Brightfield images were captured on an Olympus BX51 microscope equipped with Olympus DP-70 digital camera.

Immunofluorescence

Brain sections were prepared as above. The concentration of primary antibodies was 1:200 mouse anti-p62 (Abnova), 1:500 rabbit anti-GFAP (Abcam), 1:100 rabbit anti-TDP-43 (Proteintech Group), 1:250 rabbit anti-Iba1 (Wako Pure Chemical Industries), 1:200 rabbit anti-ubiquitin (Dako) and 1:5000 rat anti-LAMP-2 (ABL-93 concentrate). Prior to staining with anti-Iba1 and anti-LAMP-2, sections were treated with 0.2% Saponin (Sigma). Secondary detection was carried out with antibodies conjugated to Alexa 488 or Alexa 594 (Invitrogen) at dilutions of 1:500 to 1:1000. For immunofluorescence in the blue range, rabbit primary antibodies were detected with 1:500 biotin-conjugated goat anti-rabbit (Invitrogen) and 1:500 Neutravidin Alexa 350 (Invitrogen). Mouse monoclonal anti-NeuN conjugated to Alexa 488 (Millipore) was applied to sections at 1:100 after secondary detection of mouse anti-p62. Images were captured on an Olympus BX51 microscope equipped with epifluorescence and an Olympus DP-70 digital camera. Images were processed and merged using Adobe Photoshop software. A Zeiss LSM 510-META laser scanning confocal microscope was used for imaging Fig. 6D and E.

Ultrastructure

Mice were perfused with 2.5% glutaraldehyde, and tissue was processed for electron microscopy as described previously (43).

AUTHOR CONTRIBUTIONS

C.J.F., G.M.L. and M.H.M. designed experiments, analyzed results and wrote the manuscript. C.J.F. and G.M.L carried out the experiments. M.H.M. directed the project.

SUPPLEMENTARY MATERIAL

Supplementary Material is available at *HMG* online.

ACKNOWLEDGEMENTS

We thank Roman Giger for assistance with MAG *in situ* hybridization, Clement Chow and Julie Jones for preparation of tissues for electron microscopy, and Jennifer Kearney for tissue from Q54 mice. We also thank Dan Klionsky, Andrew Lieberman, Matthew Elrick and Robert Fuller for helpful discussions and critical review of the manuscript.

Conflict of Interest Statement. None declared.

FUNDING

This work was supported by NIH research grant R01 GM24872 (M.H.M.), Medical Sciences Training Program T32 GM07863 (C.J.F.), Training Program in Systems and Integrative Biology T32 GM008322 (C.J.F.) and a postdoctoral fellowship from the Hartwell Foundation (G.M.L.). Funding to pay the Open Access publication charges for this article was provided by the NIH.

REFERENCES

1. Duex, J.E., Tang, F. and Weisman, L.S. (2006) The Vac14p–Fig4p complex acts independently of Vac7p and couples PI3,5P2 synthesis and turnover. *J. Cell Biol.*, **172**, 693–704.
2. Jin, N., Chow, C.Y., Liu, L., Zolov, S.N., Bronson, R., Davisson, M., Petersen, J.L., Zhang, Y., Park, S., Duex, J.E. *et al.* (2008) VAC14 nucleates a protein complex essential for the acute interconversion of PI3P and PI(3,5)P(2) in yeast and mouse. *EMBO J.*, **27**, 3221–3234.
3. Chow, C.Y., Zhang, Y., Dowling, J.J., Jin, N., Adamska, M., Shiga, K., Szigeti, K., Shy, M.E., Li, J., Zhang, X. *et al.* (2007) Mutation of FIG4 causes neurodegeneration in the pale tremor mouse and patients with CMT4J. *Nature*, **448**, 68–72.
4. Chow, C.Y., Landers, J.E., Bergren, S.K., Sapp, P.C., Grant, A.E., Jones, J.M., Everett, L., Lenk, G.M., McKenna-Yasek, D.M., Weisman, L.S. *et al.* (2009) Deleterious variants of FIG4, a phosphoinositide phosphatase, in patients with ALS. *Am. J. Hum. Genet.*, **84**, 85–88.
5. Zhang, Y., Zolov, S.N., Chow, C.Y., Slutsky, S.G., Richardson, S.C., Piper, R.C., Yang, B., Nau, J.J., Westrick, R.J., Morrison, S.J. *et al.* (2007) Loss of Vac14, a regulator of the signaling lipid phosphatidylinositol 3,5-bisphosphate, results in neurodegeneration in mice. *Proc. Natl Acad. Sci. USA*, **104**, 17518–17523.
6. Ikonomov, O.C., Sbrissa, D. and Shisheva, A. (2006) Localized PtdIns 3,5-P2 synthesis to regulate early endosome dynamics and fusion. *Am. J. Physiol. Cell Physiol.*, **291**, C393–C404.
7. Rutherford, A.C., Traer, C., Wassmer, T., Pattni, K., Bujny, M.V., Carlton, J.G., Stenmark, H. and Cullen, P.J. (2006) The mammalian phosphatidylinositol 3-phosphate 5-kinase (PIKfyve) regulates endosome-to-TGN retrograde transport. *J. Cell Sci.*, **119**, 3944–3957.
8. Sbrissa, D., Ikonomov, O.C., Fu, Z., Ijuin, T., Gruenberg, J., Takenawa, T. and Shisheva, A. (2007) Core protein machinery for mammalian phosphatidylinositol 3,5-bisphosphate synthesis and turnover that regulates the progression of endosomal transport Novel Sac phosphatase joins the ArPIKfyve-PIKfyve complex. *J. Biol. Chem.*, **282**, 23878–23891.
9. Zhang, X., Chow, C.Y., Sahenk, Z., Shy, M.E., Meisler, M.H. and Li, J. (2008) Mutation of FIG4 causes a rapidly progressive, asymmetric neuronal degeneration. *Brain*, **131**, 1990–2001.
10. Dove, S.K., Dong, K., Kobayashi, T., Williams, F.K. and Michell, R.H. (2009) Phosphatidylinositol 3,5-bisphosphate and Fab1p/PIKfyve underPPIn endo-lysosome function. *Biochem. J.*, **419**, 1–13.
11. Klionsky, D.J. (2007) Autophagy: from phenomenology to molecular understanding in less than a decade. *Nat. Rev. Mol. Cell Biol.*, **8**, 931–937.
12. Axe, E.L., Walker, S.A., Manifava, M., Chandra, P., Roderick, H.L., Habermann, A., Griffiths, G. and Ktistakis, N.T. (2008) Autophagosome formation from membrane compartments enriched in phosphatidylinositol 3-phosphate and dynamically connected to the endoplasmic reticulum. *J. Cell Biol.*, **182**, 685–701.
13. Razi, M., Chan, E.Y. and Tooze, S.A. (2009) Early endosomes and endosomal coatomer are required for autophagy. *J. Cell Biol.*, **185**, 305–321.
14. Klionsky, D.J., Abeliovich, H., Agostinis, P., Agrawal, D.K., Aliev, G., Askew, D.S., Baba, M., Baehrecke, E.H., Bahr, B.A., Ballabio, A. *et al.* (2008) Guidelines for the use and interpretation of assays for monitoring autophagy in higher eukaryotes. *Autophagy*, **4**, 151–175.
15. Kuusisto, E., Kauppinen, T. and Alafuzoff, I. (2008) Use of p62/SQSTM1 antibodies for neuropathological diagnosis. *Neuropathol. Appl. Neurobiol.*, **34**, 169–180.
16. Wang, I.F., Wu, L.S. and Shen, C.K. (2008) TDP-43: an emerging new player in neurodegenerative diseases. *Trends Mol. Med.*, **14**, 479–485.
17. Zhang, Y.J., Xu, Y.F., Cook, C., Gendron, T.F., Roettges, P., Link, C.D., Lin, W.L., Tong, J., Castanedes-Casey, M., Ash, P. *et al.* (2009) Aberrant cleavage of TDP-43 enhances aggregation and cellular toxicity. *Proc. Natl Acad. Sci. USA*, **106**, 7607–7612.
18. Sreedharan, J., Blair, I.P., Tripathi, V.B., Hu, X., Vance, C., Rogelj, B., Ackerley, S., Durnall, J.C., Williams, K.L., Buratti, E. *et al.* (2008) TDP-43 mutations in familial and sporadic amyotrophic lateral sclerosis. *Science*, **319**, 1668–1672.
19. Kearney, J.A., Plummer, N.W., Smith, M.R., Kapur, J., Cummins, T.R., Waxman, S.G., Goldin, A.L. and Meisler, M.H. (2001) A gain-of-function mutation in the sodium channel gene Scn2a results in seizures and behavioral abnormalities. *Neuroscience*, **102**, 307–317.
20. Eskelinen, E.L., Tanaka, Y. and Saftig, P. (2003) At the acidic edge: emerging functions for lysosomal membrane proteins. *Trends Cell Biol.*, **13**, 137–145.
21. Sharkey, L.M., Cheng, X., Drews, V., Buchner, D.A., Jones, J.M., Justice, M.J., Waxman, S.G., Dib-Hajj, S.D. and Meisler, M.H. (2009) The ataxia3 mutation in the N-terminal cytoplasmic domain of sodium channel Na(v)1.6 disrupts intracellular trafficking. *J. Neurosci.*, **29**, 2733–2741.
22. Rusten, T.E., Vaccari, T., Lindmo, K., Rodahl, L.M., Nezis, I.P., Sem-Jacobsen, C., Wendler, F., Vincent, J.P., Brech, A., Bilder, D. *et al.* (2007) ESCRTs and Fab1 regulate distinct steps of autophagy. *Curr. Biol.*, **17**, 1817–1825.
23. Nicot, A.S., Fares, H., Payrastre, B., Chisholm, A.D., Labouesse, M. and Laporte, J. (2006) The phosphoinositide kinase PIKfyve/Fab1p regulates terminal lysosome maturation in *Caenorhabditis elegans*. *Mol. Biol. Cell*, **17**, 3062–3074.
24. Mizushima, N. and Yoshimori, T. (2007) How to interpret LC3 immunoblotting. *Autophagy*, **3**, 542–545.
25. de Lartigue, J., Polson, H., Feldman, M., Shokat, K., Tooze, S.A., Urbe, S. and Clague, M.J. (2009) PIKfyve regulation of endosome-linked pathways. *Traffic*, **10**, 883–893.
26. Ross, C.A. and Poirier, M.A. (2004) Protein aggregation and neurodegenerative disease. *Nat. Med.*, **10** (suppl.), S10–S17.
27. Barbeito, L.H., Pehar, M., Cassina, P., Vargas, M.R., Peluffo, H., Viera, L., Estevez, A.G. and Beckman, J.S. (2004) A role for astrocytes in motor neuron loss in amyotrophic lateral sclerosis. *Brain Res. Rev.*, **47**, 263–274.

28. Gong, Y.H., Parsadanian, A.S., Andreeva, A., Snider, W.D. and Elliott, J.L. (2000) Restricted expression of G86R Cu/Zn superoxide dismutase in astrocytes results in astrocytosis but does not cause motoneuron degeneration. *J. Neurosci.*, **20**, 660–665.
29. Lino, M.M., Schneider, C. and Caroni, P. (2002) Accumulation of SOD1 mutants in postnatal motoneurons does not cause motoneuron pathology or motoneuron disease. *J. Neurosci.*, **22**, 4825–4832.
30. Jaarsma, D., Teuling, E., Haasdijk, E.D., De Zeeuw, C.I. and Hoogenraad, C.C. (2008) Neuron-specific expression of mutant superoxide dismutase is sufficient to induce amyotrophic lateral sclerosis in transgenic mice. *J. Neurosci.*, **28**, 2075–2088.
31. Yamanaka, K., Chun, S.J., Boillee, S., Fujimori-Tonou, N., Yamashita, H., Gutmann, D.H., Takahashi, R., Misawa, H. and Cleveland, D.W. (2008) Astrocytes as determinants of disease progression in inherited amyotrophic lateral sclerosis. *Nat. Neurosci.*, **11**, 251–253.
32. Pacheco, C.D., Elrick, M.J. and Lieberman, A.P. (2009) Tau deletion exacerbates the phenotype of Niemann–Pick type C mice and implicates autophagy in pathogenesis. *Hum. Mol. Genet.*, **18**, 956–965.
33. Hara, T., Nakamura, K., Matsui, M., Yamamoto, A., Nakahara, Y., Suzuki-Migishima, R., Yokoyama, M., Mishima, K., Saito, I., Okano, H. *et al.* (2006) Suppression of basal autophagy in neural cells causes neurodegenerative disease in mice. *Nature*, **441**, 885–889.
34. Komatsu, M., Waguri, S., Chiba, T., Murata, S., Iwata, J., Tanida, I., Ueno, T., Koike, M., Uchiyama, Y., Kominami, E. *et al.* (2006) Loss of autophagy in the central nervous system causes neurodegeneration in mice. *Nature*, **441**, 880–884.
35. Brickner, J.H. and Fuller, R.S. (1997) SOI1 encodes a novel, conserved protein that promotes TGN-endosomal cycling of Kex2p and other membrane proteins by modulating the function of two TGN localization signals. *J. Cell Biol.*, **139**, 23–36.
36. Rampoldi, L., Dobson-Stone, C., Rubio, J.P., Danek, A., Chalmers, R.M., Wood, N.W., Verellen, C., Ferrer, X., Malandrini, A., Fabrizi, G.M. *et al.* (2001) A conserved sorting-associated protein is mutant in chorea-acanthocytosis. *Nat. Genet.*, **28**, 119–120.
37. Parkinson, N., Ince, P.G., Smith, M.O., Highley, R., Skibinski, G., Andersen, P.M., Morrison, K.E., Pall, H.S., Hardiman, O., Collinge, J. *et al.* (2006) ALS phenotypes with mutations in CHMP2B (charged multivesicular body protein 2B). *Neurology*, **67**, 1074–1077.
38. Filimonenko, M., Stuffers, S., Raiborg, C., Yamamoto, A., Malerod, L., Fisher, E.M., Isaacs, A., Brech, A., Stenmark, H. and Simonsen, A. (2007) Functional multivesicular bodies are required for autophagic clearance of protein aggregates associated with neurodegenerative disease. *J. Cell Biol.*, **179**, 485–500.
39. Hetz, C., Thielen, P., Matus, S., Nassif, M., Court, F., Kiffin, R., Martinez, G., Cuervo, A.M., Brown, R.H. and Glimcher, L.H. (2009) XBP-1 deficiency in the nervous system protects against amyotrophic lateral sclerosis by increasing autophagy. *Genes Dev.*, **23** [Epub ahead of print].
40. Young, J.E., Martinez, R.A. and La Spada, A.R. (2009) Nutrient deprivation induces neuronal autophagy and implicates reduced insulin signaling in neuroprotective autophagy activation. *J. Biol. Chem.*, **284**, 2363–2373.
41. Sarkar, S., Ravikumar, B., Floto, R.A. and Rubinsztein, D.C. (2009) Rapamycin and mTOR-independent autophagy inducers ameliorate toxicity of polyglutamine-expanded huntingtin and related proteinopathies. *Cell Death Differ.*, **16**, 46–56.
42. Harrison, D.E., Strong, R., Sharp, Z.D., Nelson, J.F., Astle, C.M., Flurkey, K., Nadon, N.L., Wilkinson, J.E., Frenkel, K., Carter, C.S. *et al.* (2009) Rapamycin fed late in life extends lifespan in genetically heterogeneous mice. *Nature*, **460**, 331–332.
43. Jones, J.M., Huang, J.D., Mermall, V., Hamilton, B.A., Mooseker, M.S., Escayg, A., Copeland, N.G., Jenkins, N.A. and Meisler, M.H. (2000) The mouse neurological mutant flailer expresses a novel hybrid gene derived by exon shuffling between Gnb5 and Myo5a. *Hum. Mol. Genet.*, **9**, 821–828.